


Research Article

Vibration Isolation of Existing Buildings in Microvibration Traffic Environment

Qian Xia ¹, Wen-jun Qu,² Yi-qing Li,³ and Jin Zhao³

¹School of Civil Engineering and Architecture, Xi'an University of Technology, JinHua Road 5, Xi'an 710048, China

²College of Civil Engineering, Tongji University, Siping Road 1239, Shanghai 200092, China

³Shaanxi JDWG Quality Testing Technology Co. Ltd, Yanxiang Road, Xi'an 710061, China

Correspondence should be addressed to Qian Xia; ice69pipiniu@163.com

Received 8 July 2019; Revised 12 September 2019; Accepted 26 September 2019; Published 27 October 2019

Academic Editor: Miguel Neves

Copyright © 2019 Qian Xia et al. This is an open access article distributed under the Creative Commons Attribution License, which permits unrestricted use, distribution, and reproduction in any medium, provided the original work is properly cited.

In order to explore the impact of traffic environmental microvibration on buildings, this paper studies indoor vibration isolation, a method applicable to existing buildings. The vibration isolation scheme is designed based on the residential buildings adjacent to metro lines in Shanghai. By using the dynamic theory, the effective range of vibration isolation stiffness is analyzed. The effectiveness of the indoor vibration isolation method is verified through theoretical calculations and comparison of field measurements before and after isolation. A detailed numerical model is established to analyze the indoor isolation and the effect after parameter optimization from the slab thickness, filling material, and isolator stiffness. The results show that the isolation effect is proportional to the thickness of the total slab thickness of the isolation system and inversely proportional to the stiffness of the isolator. And when concrete is used as the filling material, the isolation effect is best. The isolation effect of the midspan position is better than that of the wall-floor junction. The vibration isolation effect is more obvious after the parameters are optimized. With its convenient construction technology, short cycle, and low cost, this method is worth promoting.

1. Introduction

The impact of rail transit vibration on the work and life of residents in its surrounding buildings, as well as its influence on the normal use of precision instruments, has attracted extensive attention from academic and engineering circles [1, 2]. Recent studies on vibration isolation technology in existing buildings focus mainly on the application and research of several isolation methods. Each has its own advantages and problems. The floating floor vibration isolation technology [3] and the room-in-room vibration isolation technology [4] have high headroom requirements on the houses. They are mainly used in buildings with considerable headroom such as concert halls and theaters. The overall vibration isolation technology [5, 6] has good effect, but costs are high for the existing buildings. It is mostly used for planned buildings or existing buildings with historic value. Because of such factors as headroom and cost, none of the three technologies

is applicable to common existing buildings, especially those with the old-fashioned masonry residential structure. The indoor vibration isolation method proposed in this paper is specifically designed for existing buildings and can meet the headroom requirements. Qu Wenjun and Xia Qian's research team first proposed this method conducted preliminary research [7, 8] and discovered its significant isolation effect. So far, no better method has been proposed by other research teams which is more suitable for existing buildings nor has any team conducted researches to improve this method. By analyzing the vibration reduction effect, combined with structural dynamics theory, this paper analyzes the effective range of vibration isolation stiffness and has proved the effectiveness of the indoor vibration isolation method practically and theoretically. The isolation effect of the method is analyzed in terms of three factors: floor thickness, filling material, and isolator stiffness, so as to provide data support for the promotion of the method in the future.

2. Determination of the Vibration Isolation Scheme

2.1. Overview of the Test Buildings. A section of metro lines in Shanghai is chosen for the test, with two common masonry-structured residential buildings on the site. This paper takes Building 2 as the research object, as shown in Figure 1. The building is a 5-storey masonry structure, 10 meters from the subway central line. Built in the 1960s, it is light in weight and poor in structural integrity, so it will have strong response to external vibrations. The planimetric relationship between the building and the tunnel is shown in Figure 2.

2.2. Introduction to the Vibration Isolation Method. First proposed by the authors' research team, the indoor vibration isolation method is a new type of vibration reduction technology for existing buildings in subway areas. Based on the principle of structural dynamics, the indoor ground vibration characteristics, and the structural features of the house, the balance and stability of the indoor ground and house structure are all taken into account to establish a practical method for estimating the isolation efficiency of the system. The following isolation technology and corresponding technical parameters are proposed: to excavate the ground floor of each room of the existing building (the excavation depth being no less than 200 cm), the backfill is tamped, and on top of the tamped backfill, three structural layers are made from bottom to top:

- (1) The bottom layer is the core layer composed of the rubber vibration isolator which may as well be made of special compounded rubber synthesized from high-strength metal thin layers (laminated). The static stiffness K_{zs} of the rubber is calculated according to equation (1), with rubber height greater than 30 mm and width greater than 150 mm × 150 mm. The number of vibration isolators and layout spacing are determined by the specific project (the recommended vibration isolator spacing is less than 500 mm). The overall height of the core layer is greater than 30 mm:

$$\frac{W_1}{N} \frac{1}{K_{zs}} < \rho \text{ (mm)}, \quad (1)$$

where W_1 , N , and ρ stand for the indoor dynamic load, the number of vibration isolators, and the ground subsidence control displacement, respectively.

- (2) The middle layer is a C20 plain concrete layer with thickness greater than 100 mm.
- (3) The top layer is the ordinary indoor floor, which should be built 24 hours after the pouring of the middle layer.

The gaps between the three structural layers are filled with polymer foam boards. Based on the dynamic principle of vibration isolation, with the balance and stability of the

structure considered, a ground vibration isolation scheme is proposed, as shown in Figure 3. Each room is an independent isolation system consisting of a floor and a set of isolators.

2.2.1. Characteristics and Difficulties in the Vibration Isolation. Structural vibration isolation is realized by reducing the frequency of the isolation system consisting of an isolator and a structure, thereby reducing the structure's response to input vibrations above (or equal to) this frequency. The relationship between the vibration frequency and the system quality is expressed as

$$f_n = \frac{1}{2\pi} \sqrt{\frac{K_z}{M}}, \quad (2)$$

where f_n , M , and K_z are the frequency (Hz), mass (kg), and dynamic stiffness (N/m) of the vibration isolation system, respectively. The indoor floor of the building must stay vertically stable every day; that is, the system is supposed to have considerable stiffness. From equation (2), it can be seen that, at a constant frequency, the larger the mass, the higher the stiffness of the system. When the horizontal area of the structure is constant, the vertical height of the system is determined by its mass. For the existing buildings, generally, the superstructure and foundation have become an unchangeable one. In order to maintain the integrity of the structure without increasing the load of the foundation, the space height left for vibration isolation in the room is very limited. In addition, to maintain the balance and multidirectional stability of the indoor floor, it is usually necessary to establish an isolation system composed of multiple isolators. The quality of the isolation system is normally proportional to the number of isolators, which further increases the limitation of the structural space on the quality configuration of the system. Because of the horizontal vibration caused by the subway, the indoor vibration isolation of the building is different from that of other places. The requirements for the lateral and vertical stability of the ground structure are also high.

2.2.2. Vibration Isolation Technology Selection and Arrangement of Isolators. To study and design the vibration isolation system, one must first analyze and select the type of isolation technology. Based on the actual situation of the test building, the performance and application scope of common isolation technologies are as follows:

- (1) According to the stability requirement of the structure, it is not advisable to use steel springs and fiberglass as the vibration isolation material.
- (2) Air springs are not suitable for vibration isolation of ordinary houses because of their complicated structure and high price.
- (3) Considering the practical use and the convenience of material processing, we have selected artificial rubber to make isolation devices for the test building.

The number of isolators and their spacing are determined by specific projects. It is recommended that the



FIGURE 1: Test building. (a) North side. (b) South side.

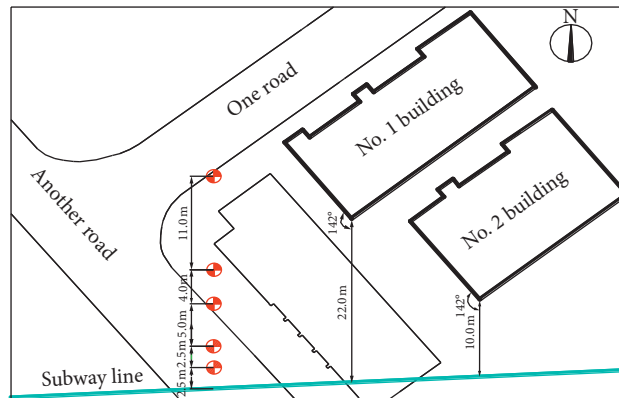


FIGURE 2: Planimetric relationship between the building and the tunnel.

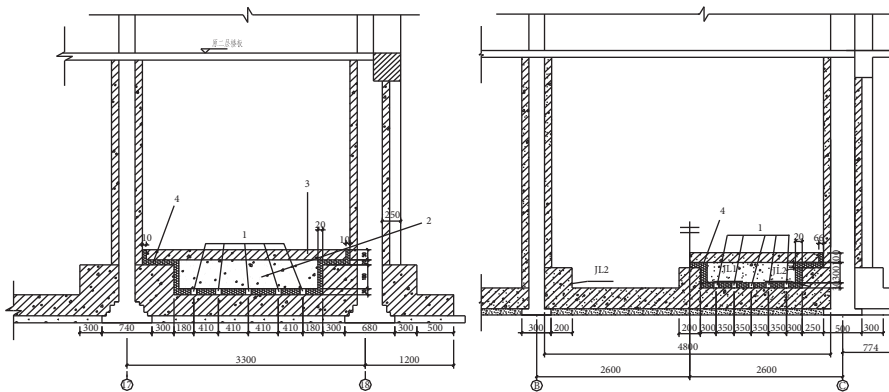


FIGURE 3: Cross section of the vibration isolation system. Note. 1: rubber vibration isolator; 2: C20 plain concrete layer; 3: ordinary indoor floor; 4: polymer foam board.

spacing between isolators be less than 500 mm and the overall height of the core layer be greater than 30 mm. Based on the above parameters, the isolators are arranged in every room of the test building (the name and location of each room are shown in Figure 4). Figure 5 shows the layout of the isolators in Room SN2.

3. Theoretical Basis of Vibration Isolation

3.1. Parameter Calculation. The indoor ground vibration isolation system of existing buildings is a single-degree-of-

freedom system. Its main characteristic parameters include the system's natural vibration frequency, static stiffness, and mass. The above parameters are determined after considering the external vibration characteristics, the dynamic performance, and the structural characteristics of the vibration isolation material. The detailed theoretical analysis is as follows.

3.1.1. Dynamic Range of Natural Vibration Frequency and Vibration Isolation Coefficient. Suppose the vertical input

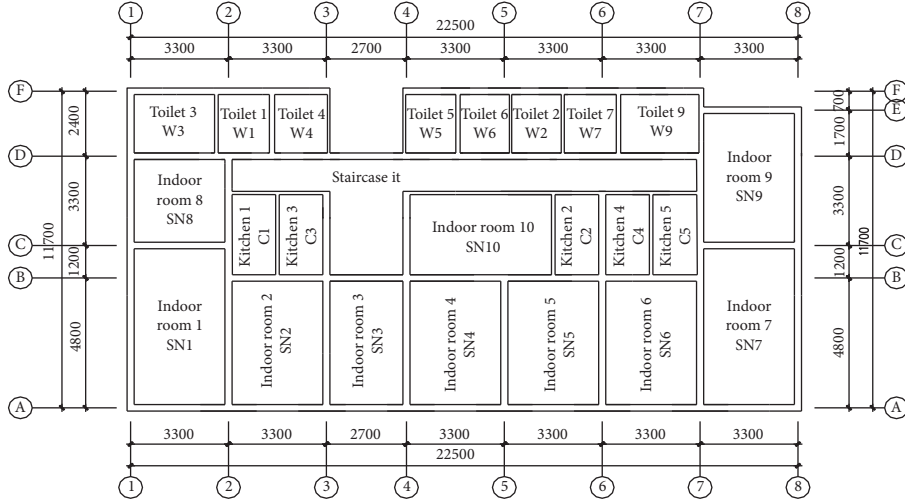


FIGURE 4: Name and location of each room.

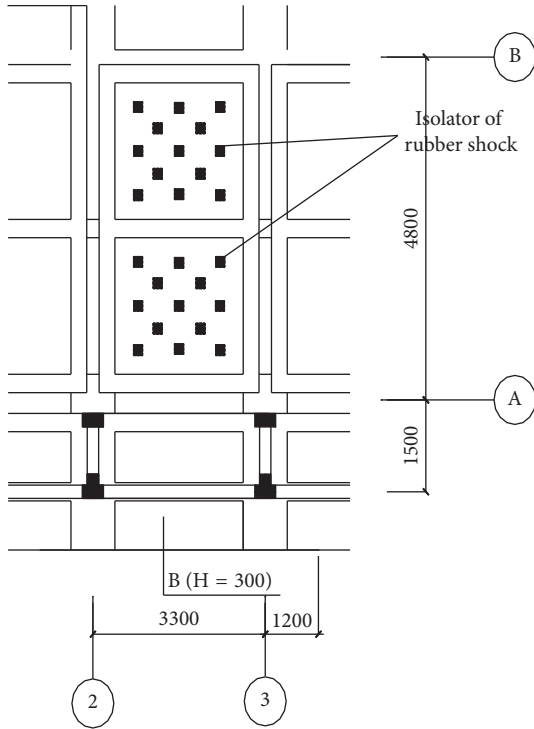


FIGURE 5: Arrangement of isolators in Room SN2.

vibration frequency of the house ground caused by subway is $\lambda = (78.5 \times 10/26)(1/K_{zs}) < 0.1$, and the natural frequency of vertical vibration of the vibration isolation system is f_n . If $f_a/f_n \geq \sqrt{2}$, then the system has vibration isolation effect for any input vibration with a frequency greater than $\lambda = (78.5 \times 10/26)(1/K_{zs}) < 0.1$. Normally, the following relation is satisfied:

$$\sqrt{2} \leq \frac{f_a}{f_n} \leq 5. \quad (3)$$

The isolation coefficient η is

$$\eta = \sqrt{\frac{1 + 4\xi^2(f^2/f_n^2)}{(1 - (f^2/f_n^2))^2 + 4\xi^2(f^2/f_n^2)}}, \quad (4)$$

where $f > f_a$ and ξ is the damping ratio of the vibration isolation system, which is 0.1. The vibration isolation efficiency T is

$$T = (1 - \eta) \times 100\%. \quad (5)$$

The related literature [7] proposed a method for estimating the efficiency of the vibration isolation system based on the isolation coefficient corresponding to the lower cutoff frequency of the maximum acceleration level of 1/3 octave, which is used as the vibration isolation frequency of the vibration isolation system. Combined with the measured vibration results of test building No. 2 without isolation measures, the maximum acceleration level of 1/3 octave of the ground floor room is measured to be at the center frequency of 50 Hz (see references [8–10]). The corresponding lower cutoff frequency is the frequency of the vertical input vibration of the ground, that is, $f_a = 44.7$ Hz. According to equation (3), we have

$$8.94 \leq f_n \leq 31.6. \quad (6)$$

The vibration isolation coefficient and isolation efficiency are

$$\eta_a = \sqrt{\frac{1 + 4\xi^2(f_a^2/f_n^2)}{(1 - (f_a^2/f_n^2))^2 + 4\xi^2(f_a^2/f_n^2)}}, \quad (7)$$

$$T_a = (1 - \eta_a) \times 100\%. \quad (8)$$

It is obvious that

$$\begin{aligned} \eta &< \eta_a, \\ T_a &< T. \end{aligned} \quad (9)$$

According to equations (4) and (5), for the isolation coefficient η_0 and the vibration isolation efficiency T_0 corresponding to the center frequency of the 1/3 octave of the isolation system, we also have

$$\begin{aligned}\eta_0 &< \eta_a, \\ T_a &< T_0.\end{aligned}\quad (10)$$

After vibration isolation treatment, the maximum acceleration level of 1/3 octave L_{a0} is

$$L_{a0} < 99\eta_0. \quad (11)$$

3.1.2. System Mass M and Isolator Height H . A trial method is used for calculation. The vertical deformation of the system is not considered, and the mass of the vibration isolator is omitted. The system mass is

$$M = |S_1(D - H) + S_2d|\gamma_c, \quad (12)$$

where S_1 is the floor excavation area of the room, D is the excavation height, S_2 is approximately the room area, d is the room floor thickness, H is the isolator height, and γ_c is the specific gravity of the ground material.

Taking Room SN2 as an example, based on its net size, $S_1 = 13.9 \text{ m}^2$, $D = 0.2 \text{ m}$, $S_2 = 13.9$, and $d = 0.1 \text{ m}$. The ground material is supposed to be concrete, and the corresponding $\gamma_c = 2100 \text{ kg/m}^3$. When H takes the typical value of 3 cm, M is calculated to be around $7.9 \times 10^3 \text{ kg}$ according to equation (12). Each vibration isolator in the system is subjected to a weight of $7.9 \times 10^3 \text{ kg}/26 = 303.8 \text{ kg}$ (26 vibration isolators are arranged in Room SN2).

3.1.3. Static Stiffness of the Vibration Isolation System K_{zs} . Assume a total of ten people with an average weight of 80 kg are simultaneously moving in a room at the same time (this situation is rare in reality). Considering the stability of structure, the vertical displacement of the floor should be

$$\lambda = \frac{80 \times 9.8 \times 10}{26} \frac{1}{K_{zs}} < 0.1 \text{ (mm)}. \quad (13)$$

According to equation (13), we find $K_{zs} = 3.02 \times 10^4 \text{ N/cm}$ (minimum value). As shown in Figure 5, there are 26 isolators arranged in the room.

3.1.4. Dynamic Stiffness K_z and System Natural Frequency f_n . The dynamic stiffness of the system is

$$K_z = n_d K_{zs}, \quad (14)$$

where n_d stands for the ratio of the dynamic stiffness to the static stiffness of the rubber material, which is 2.5 [11]. We have

$$K_z = 7.54 \times 10^4 \text{ (N/cm)}. \quad (15)$$

Substituting the value of K_z and the weight borne by each isolator (303.8 kg) into equation (2) yields $f_n = 25.1 \text{ Hz}$, which clearly satisfies the requirements of equation (6).

3.1.5. Vibration Isolation Effect of the System. According to equations (7), (10), and (11), we have

$$\begin{aligned}\eta_0 < \eta_a &= \sqrt{\frac{1 + 4 \times 0.1^2 \times (44.7^2/25.1^2)}{(1 - (44.7^2/25.1^2))^2 + 4 \times 0.1^2 \times (44.7^2/25.1^2)}} \\ &= 0.482 \approx 48\%,\end{aligned}$$

$$T_0 > |1 - \eta_a| = 52\%,$$

$$L_{a0} < 99\eta_0 = 48 \text{ dB}.$$

(16)

After adopting the vibration damping scheme, the maximum acceleration level of 1/3 octave with a center frequency of 50 Hz is 38 dB lower than the corresponding limit (86 dB) in Standards for Indoor Vibration Limits and Measurement Methods for Residential Buildings (GB/50355-2005) [12] (Level 1 daytime limit). As can be seen, this method improves the vibration isolation effect obviously in the frequency range with 50 Hz as the center.

3.2. Stiffness Check. From equation (2), it follows that

$$K = (2\pi f)^2 \times M. \quad (17)$$

According to equation (12), if the excavation area is consistent with the room area, the system mass is $M = S|D - H + d|\gamma_c$ and the mass per unit area is $M/S = |D - H + d|\gamma_c$. Combined with equation (17), the stiffness per unit area can be obtained:

$$\frac{K}{S} = (2\pi f)^2 |D - H + d|\gamma_c. \quad (18)$$

Then, equation (6) is used to calculate relevant parameters of the vibration isolation measures for the test building (see Section 2.1 for specific values), and we have

$$1.8 \text{ kN/mm/m}^2 \leq K/S \leq 22.4 \text{ kN/mm/m}^2. \quad (19)$$

Equation (19) shows a reasonable range of stiffness per unit area when the vibration isolation system based on relevant parameters of the test buildings meets isolation requirements.

Room SN2 with a net size of 2.9 m × 4.8 m, as shown in Figure 5, is equipped with 26 vibration isolators. Theoretical calculations show that the dynamic stiffness of each isolator is 7.54 kN/mm and the stiffness per unit area is 14.1 kN/mm/m². Therefore, the arrangement of the rubber isolators used in the vibration isolation measures and the selection of isolation parameters are reasonable and meet the related requirements.

4. Comparative Analysis of Vibration Tests before and after Isolation

The indoor vibration isolation method is applied to test buildings. Under the same environment, the research team conducts on-site testing of the buildings and compares the data of each test room before and after the application of the isolation method.

4.1. Arrangement of the Test Points. In order to compare the vibration isolation effect, three typical rooms (indoor room 2 (SN2), bathroom 2 (W2), and kitchen room 2 (C2)) are selected on each floor for testing, and their locations are shown in Figure 4. Sensors are installed on the floor of each room to test the vertical (Z-direction) and horizontal (X along the longitudinal direction of the house and Y along the lateral direction of the house) isolation. SN2 and C2 are precast slab rooms, and W2 is a cast-in-place slab room. Because of the limited number of sensors, group tests are performed on vertical and horizontal vibrations of the buildings.

French Lens piezoelectric acceleration sensors (LC0132T) with a sensitivity coefficient of 49 V/g and an intelligent data acquisition system are used in the tests. All instruments and sensors have been debugged and calibrated before testing.

The test data are filtered, and acceleration signals are recorded. The vibration response of buildings is analyzed by evaluating the parameter vibration acceleration and the acceleration level.

4.2. Analysis of Vibration Isolation Effects. Because of space limitations, Figure 6 only shows the comparison of vertical vibration between the slab midspan and the junction of Room SN2. For the midspan, the vertical vibration level of the floor before isolation increases with the floor height, and the vertical vibration level of each floor after isolation is slightly attenuated as compared with that before isolation. The maximum vibration isolation is 3.26 dB on the top floor (Figure 6(a)). For the junction, the vertical vibration level of each floor after isolation is slightly attenuated as compared with that before isolation, and the isolation decreases with the floor height (Figure 6(b)). The isolation of the third to fifth floors is significantly smaller than that of the corresponding midspan, and the maximum isolation is 2.31 dB on the ground floor. It can be seen that both the midspan and the junction show obvious isolation effects. The higher the floor, the more obvious the vibration isolation effect of the midspan position as compared with the junction.

The vertical vibration levels of the three rooms are listed in Table 1. The vertical vibration levels of each floor before and after isolation can be visually observed. In indoor rooms, the vertical isolation of the midspan increases with the floor height, while it is opposite for the junction. In the kitchen room, the vertical isolation of the midspan and the junction decreases as the floor height increases. In bathrooms, the vertical isolation of the midspan and junction increases with the floor height.

The comparison of the vibration isolation of each floor is shown in Table 2. It can be seen that, on each floor, the vibration levels of different positions in the room are obviously different. For indoor rooms with a large span and kitchens and bathrooms with a small span, the isolation level of the midspan is greater than that of the wall-floor junction. The span has no obvious impact on the difference in the isolation level of each floor, and the same is true for the floor material.

The horizontal vibration level of the slab is small before and after isolation, mostly below 2 dB. Therefore, the specific values of the horizontal vibration level are not detailed here.

In order to further understand the frequency range of the damping effect and clearly reflect the isolation effect at different frequencies, the vertical vibration acceleration levels (VALs) before and after isolation are listed in Figure 7. Because of space limitations, only the information on Room SN2 on the second floor is presented.

It can be seen that the vibration reduction at the midspan position is obvious in each frequency range, with the maximum being 15.8 dB. The vibration reduction at the wall-floor junction is obvious in the frequency ranges of 2.5~6.3 Hz and 10 Hz~25 Hz, with the maximum being 11.6 dB, which is slightly smaller than that of the midspan position. Therefore, the isolation effect of the method is obvious.

5. Numerical Study of Various Parameters of the Vibration Isolation Method

In order to further analyze the effect of the indoor vibration isolation method, Room SN2 is selected as the research object; the location of the room is 10 m away from the middle line of the tunnel with its finite element model established by using ANSYS. The isolation effect is studied from slab thickness, filling material, and isolator stiffness. The vibration isolation system floor uses the SHELL181 unit, which gives the corresponding backfill material properties. The vibration intensity of the surface (10 m away from the center line of the tunnel) of the No. 2 test building is used as the model excitation, as shown in Figure 8, and the vertical vibration level is 54.8 dB [8].

The calculation of the vibration isolation floor is shown in Figure 9. The concrete slab thickness on the rubber support consists of two parts: (1) the excavation depth (cast slab thickness), which is 0.2 m, i.e., $D=0.2$ m in equation (12), and (2) the floor thickness, which is 0.1 m, i.e., $d=0.1$ m in equation (12). In order to simplify the calculation, the excavation area is approximated to be the same as the room area and the slab uses the axis size. The vertical stiffness of the isolator is 7.54, which is calculated according to the theory in Section 2.1. Because of space limitations, only the numerical model of the isolation floor with a total thickness of 0.3 m is presented, as shown in Figure 10.

The concrete strength is Grade C20, and the compressive strength takes the designed value $f_c = 9.6$ MPa. The material properties are shown in Table 3.

5.1. Analysis of the Isolation Effect for Different Thickness. A numerical model of the concrete slab with a total thickness of 0.25 m, 0.3 m, and 0.4 m is established.

Take the isolation floor with a total thickness of 0.3 m as an example. The vibration characteristics of the midspan, the upper junction, the lower junction, the left junction, and the right junction (numbered 1, 2, 3, 4, and 5) are analyzed, respectively. Figure 8 shows the comparison of excitation and response at Position 1. It can be seen that the isolation

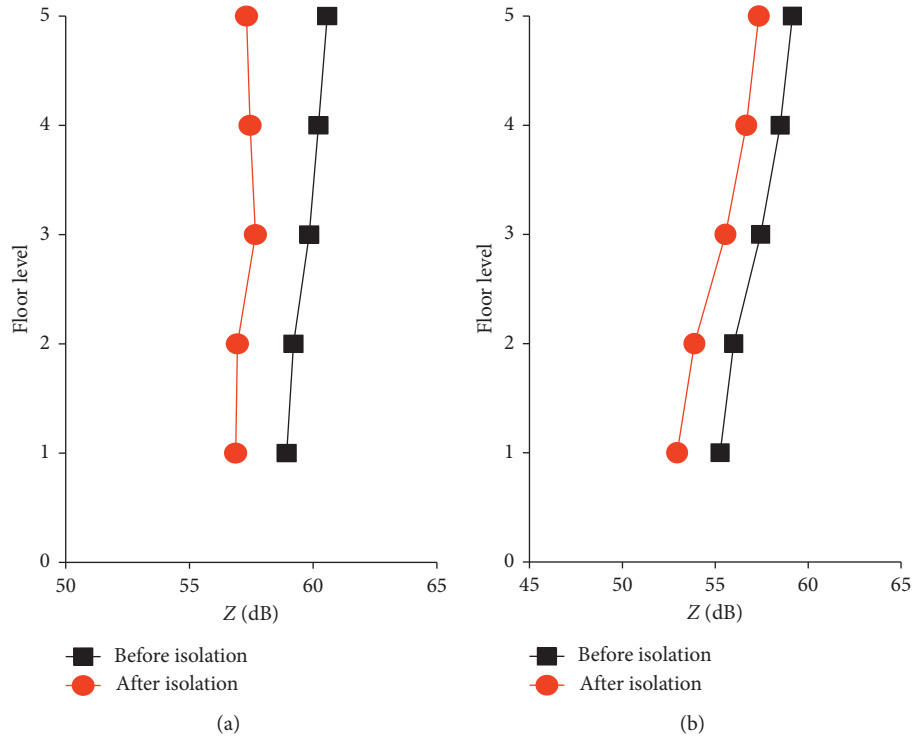


FIGURE 6: Vertical vibration level change of Room SN2 with the floor height before and after isolation. (a) Midspan. (b) Wall-floor junction.

TABLE 1: Vibration of the midspan and wall-floor junction of typical rooms before and after isolation (dB).

Room	Midspan			Wall-floor junction		
	Before isolation	After isolation	Reduction	Before isolation	After isolation	Reduction
SN2						
First	58.93	56.87	2.06	55.26	52.95	2.31
Second	59.20	56.94	2.26	56.00	53.88	2.11
Third	59.84	57.67	2.17	57.44	55.55	1.89
Fourth	60.22	57.45	2.77	58.50	56.67	1.83
Fifth	60.57	57.31	3.26	59.16	57.35	1.81
C2						
First	58.31	54.28	4.03	55.04	52.72	2.32
Second	58.56	55.45	3.11	56.58	54.29	2.29
Third	59.89	57.47	2.42	58.30	56.18	2.12
Fourth	61.04	58.62	2.41	59.35	57.26	2.09
Fifth	61.66	59.30	2.36	59.89	57.82	2.08
W2						
First	56.07	54.59	1.48	54.96	53.86	1.10
Second	56.71	54.89	1.82	55.66	54.00	1.65
Third	57.78	55.72	2.06	56.77	54.87	1.90
Fourth	58.38	55.54	2.84	57.67	55.64	2.04
Fifth	59.14	55.96	3.18	58.32	56.20	2.12

TABLE 2: Isolation difference between different floors of typical rooms.

Isolation difference of each floor	Midspan	Wall-floor junction	Evaluation of isolation effects
Indoor room	0.1 dB~0.6 dB	0.06 dB~0.22 dB	The isolation level of each floor at the midspan differs greatly, and the difference is small at the junction
Kitchen (precast slab)	0.1 dB~0.9 dB	0.03 dB~0.17 dB	The isolation level of each floor at the midspan differs greatly, and the difference is small at the junction
Bathroom (cast-in-place slab)	0.24 dB~0.78 dB	0.08 dB~0.55 dB	The isolation level of each floor at the midspan differs greatly, and the difference is relatively large at the junction

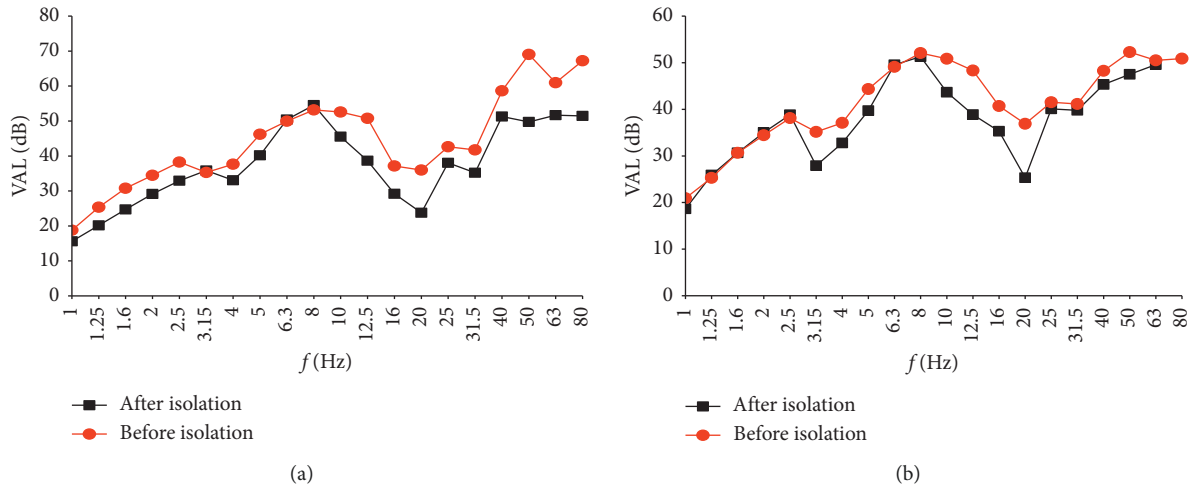


FIGURE 7: Vibration acceleration levels of Room SN2 on the second floor before and after isolation. (a) Midspan. (b) Wall-floor junction.

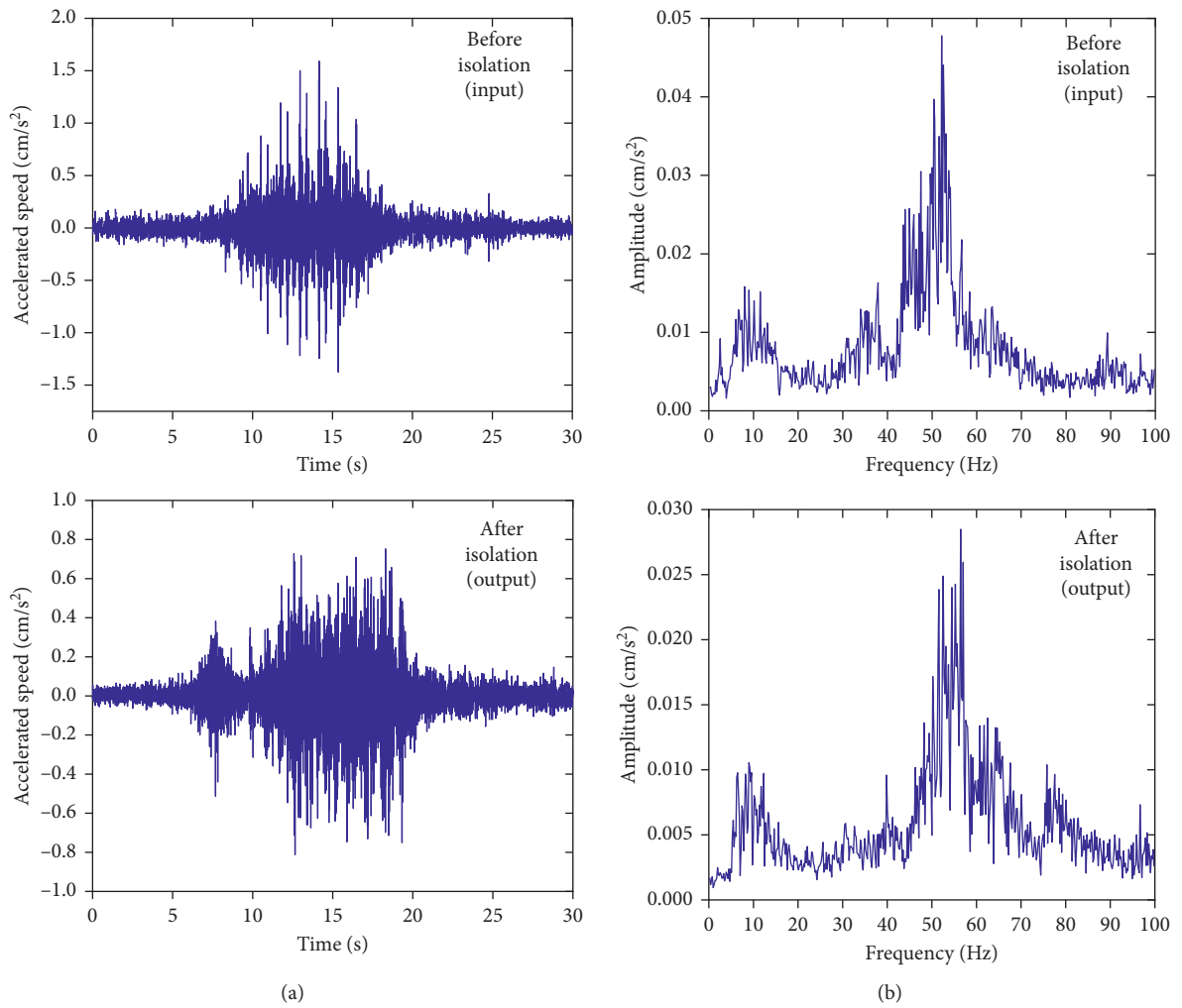


FIGURE 8: Comparative analysis of excitation and response of the isolation slab (0.3 m) at the midspan. (a) Acceleration-time history graph. (b) Spectrogram.

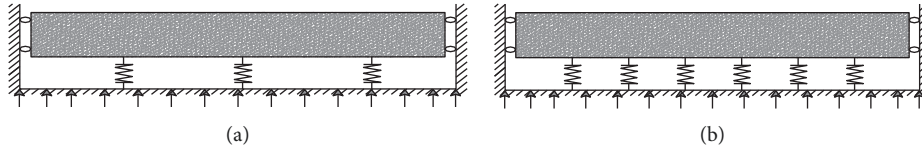


FIGURE 9: Simplified calculation of the isolation slab. (a) A-A cross section. (b) B-B cross section.

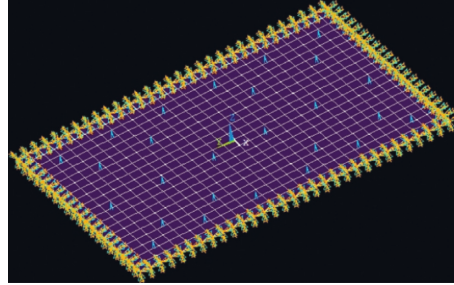


FIGURE 10: Calculation model of the isolation slab (arrowheads represent the support).

TABLE 3: Material properties.

Material	Initial elastic modulus (MPa)	Poisson's ratio	Density (kg/m ³)	Damping ratio	Strength (MPa)
Concrete	0.912×10^4	0.2	2500	0.1	9.6

effect of the scheme is obvious, mainly in the frequency range of 40~60 Hz, while in the range of 10~20 Hz, the effect is not obvious because it is close to the natural frequency of the system.

Figure 11 shows that the vibration reduction at the midspan position with a center frequency of 50 Hz is 35 dB, similar to the calculated value in Section 2.1. For both the midspan and the wall-floor junctions, the isolation effect of the 40~60 Hz frequency band is better than that of medium- and low-frequency bands.

The Z vibration level at different positions of the floor is shown in Table 4. The results show that the isolation effect is better at the midspan position, while the effect is worse at the junctions. From the perspective of the rubber support arrangement, there are more supports at the center positions. Therefore, the more vertical constraints the floor is subjected to, the better the isolation effect. The slab at the wall-floor junction is subject to little constraint, and thus, the isolation effect is poor. When the slab thickness is less than 0.4 m, the isolation effect at the midspan and wall junctions is both proportional to the thickness, and the vibration reduction is 5.3~13.2 dB and 2.5~9.3 dB, respectively.

5.2. Analysis of the Isolation Effect for Different Filling Materials. Table 5 lists the material parameters under three working conditions. Reference [13] is referred to for the concrete parameters, and the Shanghai soft soil parameters are referred to for the soil parameters, as shown in Table 6. Slabs with a total thickness of 0.3 m are used in all the three working conditions. It should be noted that the filling materials in working condition 3 are concrete and soil, which are filled in two layers with a thickness of 0.1, as shown

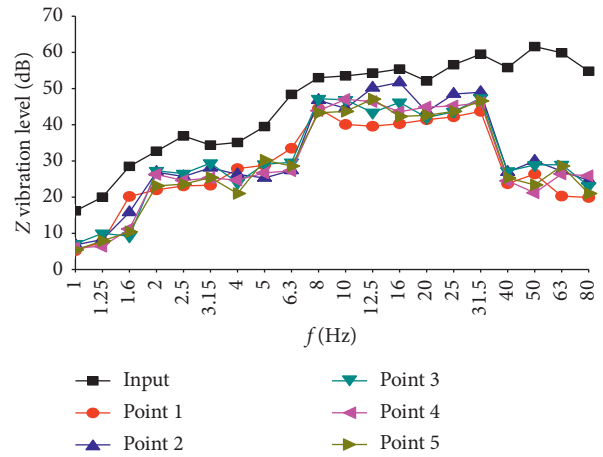


FIGURE 11: Vibration acceleration level comparison for different positions of the indoor slab (0.3 m).

in Figure 12. The excitation applied is the same as that in Section 4.1 when the isolation effect for different slab thickness is discussed.

Five positions of the slab are selected (the same as those in Section 4.1) to analyze the isolation effect under different working conditions. The results of vibration level distribution are shown in Table 7. It is found that, in condition 1 and condition 3, the isolation effect at the midspan is better than that at the wall junction. The difference in the isolation effect between the two positions under condition 1 is between 2.7 and 7.8 dB, and the difference is between 3.3 and 4.6 dB under condition 3. Under condition 2, the isolation effect at the midspan is not as obvious as that at the wall junction, but the difference is not large, ranging from 1.5 to 5.1 dB.

TABLE 4: Z vibration level distribution at different positions of the slab (/dB).

Point	Input position	1 (midspan)	2 (upper junction)	3 (lower junction)	4 (left junction)	5 (right junction)
Thickness of 0.25 m	54.8	49.5	52.3	51.7	50.9	49.4
Thickness of 0.3 m	54.8	47.0	52.1	50.6	49.6	48.5
Thickness of 0.4 m	54.8	41.6	47.1	46.3	46.1	45.5

TABLE 5: Calculation conditions of the numerical model.

Working condition no.	1	2	3
Filling material	Concrete	Soil	Concrete and soil
Poisson's ratio	0.2	0.29	Respective Poisson's ratio
Damping ratio	0.1	0.02	Respective damping ratio
Elastic modulus (N/mm ²)	0.912 × 10 ⁴	54.4	Respective elastic modulus
Density (kg/m ³)	2000	1800	Respective density

TABLE 6: Physical and mechanical parameters of soil in Shanghai.

Soil name	Bottom layer depth (m)	Gravity (KN/m ³)	Poisson's ratio	Average velocity of shear wave (m/s)	Elasticity modulus (MPa)	Shear modulus (MPa)
Soil filling	1.53	19.0	0.29	110	54.4	21.1

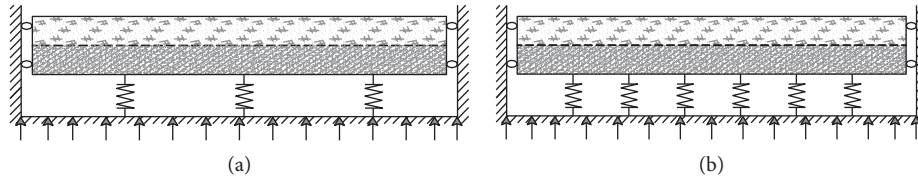


FIGURE 12: Simplified calculation of the vibration isolation slab. (a) A-A cross section. (b) B-B cross section.

TABLE 7: Z vibration level distribution at different positions of the slab under various conditions (/dB).

Point	Input position	1 (midspan)	2 (upper junction)	3 (lower junction)	4 (left junction)	5 (right junction)
Condition 1	54.8	47.0	52.1	50.6	49.6	48.5
Condition 2	54.8	54.8	51.3	52.5	51.9	53.9
Condition 3	54.8	50.2	51.5	51.1	50.6	51.4

Because of space limitations, only Point 1 and Point 4 vibration acceleration levels of the midspan and wall junction under various working conditions are listed here, as shown in Figure 13. As can be seen from Figure 13(a), the isolation effect is best when the filling material is concrete in condition 1, mainly between 40 and 80 Hz. The worst one is when the filling material is soil in condition 2, and the isolation effect is not significantly different in each frequency band. Even in the range of the 10~25 Hz intermediate frequency, vibration amplification occurs. According to Figure 13(b), in the high-frequency band (40~80 Hz), condition 1 shows the best isolation effect. In the intermediate- and low-frequency bands, the isolation effect under the three conditions is similar, with condition 1 showing the highest effect. At the center frequency of 12.5 Hz, the isolation effect in conditions 2 and 3 is slightly higher than that in condition 1. The reason might be that the frequency is close to the natural frequency of the isolation system in condition 1, which causes the resonance of the vibration isolation system.

5.3. Analysis of the Isolation Effect for Different Stiffness. The slab size of Room SN2 is 2.9 m × 4.8 m. The reasonable stiffness of a single isolator is calculated to be in the range of 0.95~12.0 kN/mm. We take 3 kN/mm, 7.54 kN/mm, and 12 kN/mm for comparative analysis, which are numbered Stiffness 3, Stiffness 7.54, and Stiffness 12. The total thickness of the slab selected is 0.3 m, and the filling material is concrete. The same five positions as before are analyzed.

The results of the vibration level distribution under various conditions are shown in Table 8. As can be observed, the smaller the stiffness, the better the isolation effect. When the stiffness is 3 kN/mm, the isolation at the midspan is 10.1 dB and the isolation at the junction positions is 6.4~9.8 dB. When the stiffness is 12 kN/mm, the isolation at the midspan is 4.4 dB and the isolation at the junction positions is 2~4.2 dB. From the perspective of the rubber support arrangement, there are more supports at the center positions. Therefore, the more vertical constraints the floor is subjected to, the better the isolation effect.

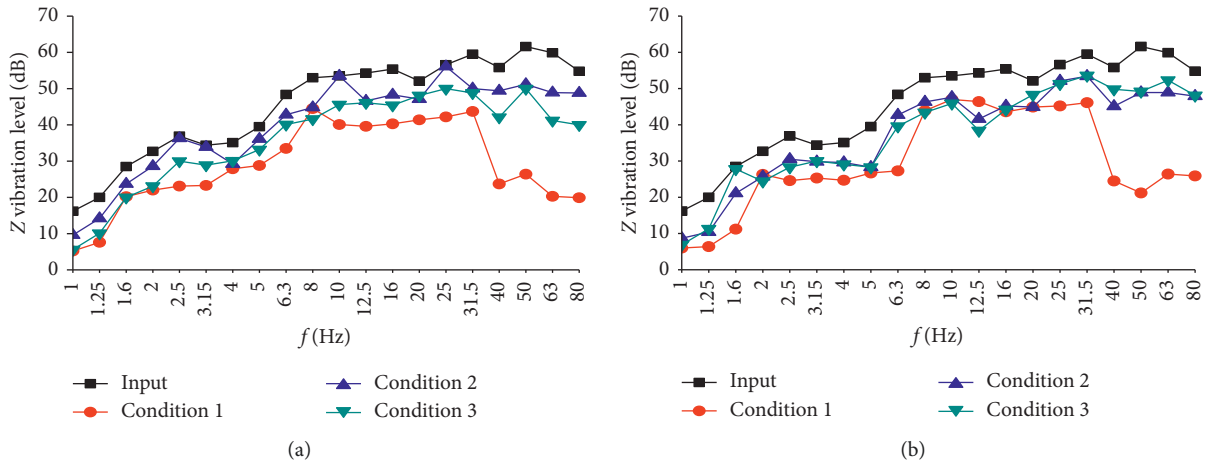


FIGURE 13: Comparison of vibration acceleration levels in various conditions. (a) Midspan. (b) Wall-floor junction.

TABLE 8: Z vibration level distribution at different positions of the slab for various stiffness (/dB).

Point	Input position	1 (midspan)	2 (upper junction)	3 (lower junction)	4 (left junction)	5 (right junction)
Stiffness 3	54.8	44.7	48.3	48.4	45.4	45.0
Stiffness 7.54	54.8	47.0	52.1	50.6	49.6	48.5
Stiffness 12	54.8	50.5	52.6	52.8	51.3	50.6

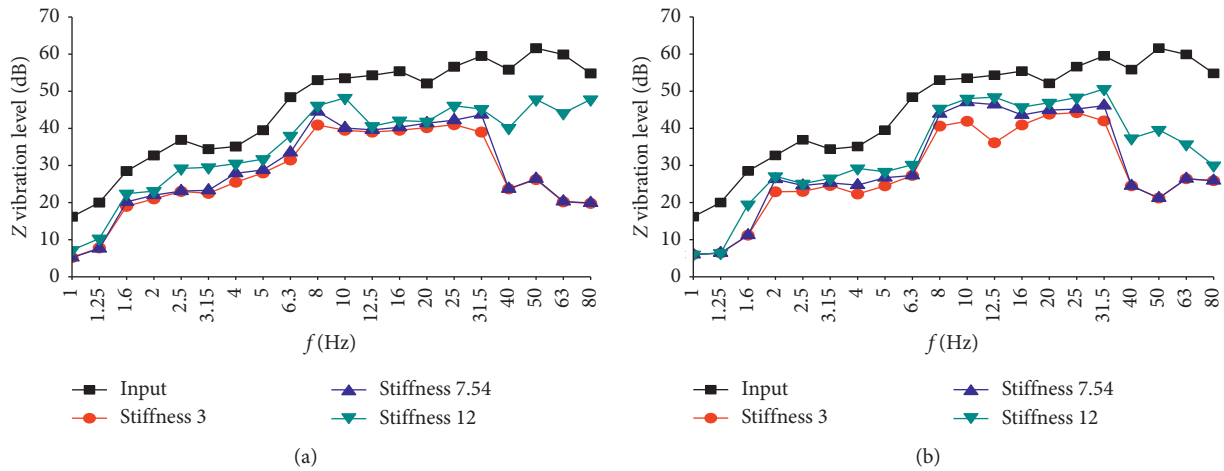


FIGURE 14: Comparison of vibration acceleration levels under different stiffness. (a) Midspan. (b) Wall-floor junction.

TABLE 9: Z vibration level distribution at different positions after parameter optimization (dB).

Input	1 (midspan)	2 (upper junction)	3 (lower junction)	4 (left junction)	5 (right junction)
54.8	38.8	43.7	44.1	42.8	42.4

Because of space limitations, only Point 1 and Point 4 vibration acceleration levels of the midspan and wall junction under different stiffness are listed here, as shown in Figure 14. As can be seen in Figure 14(a), Stiffness 3 has the best isolation effect, mainly between 40 and 80 Hz, and the worst is Stiffness 12. According to Figure 14(b), in the high-frequency band (40~80 Hz), Stiffness 3 and Stiffness 7.54 show good isolation effect, with no major difference. For Stiffness 12, its isolation effect decreases considerably. In the

intermediate- and low-frequency bands below 40 Hz, Stiffness 3 has the best isolation effect, but the difference between the three is not large.

5.4. Effect Analysis of the Isolation Method after Parameter Optimization. Based on the preceding three-parameter analysis, Room SN2 is taken as the research object. The optimized parameters are selected; that is, the total slab

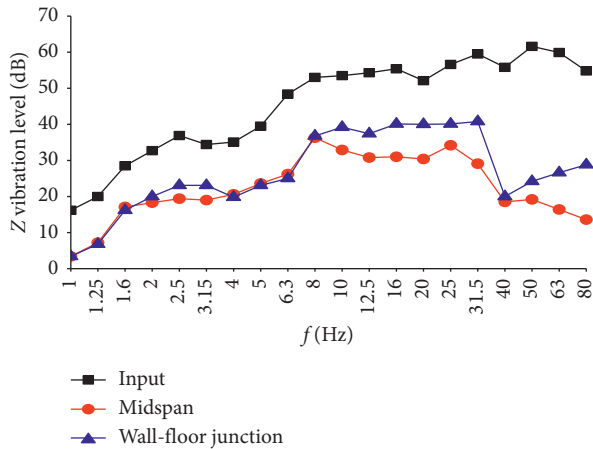


FIGURE 15: Comparison of midspan and wall-floor junction vibration acceleration levels before and after isolation.

thickness of the room is 0.4 m (including the thickness of the slab $d=0.1$ m and the cast slab thickness $D=0.3$ m; the variable names are shown in equation (12)). The filling material is concrete, and the stiffness of the isolator is 3 kN/mm (26 isolators are arranged in the room, and the reasonable stiffness of a single isolator is 1.3~16.4 kN/mm; see Section 2.2 for the calculation method). The calculation results before and after isolation are shown in Table 9, and the numbering of the five positions is the same as before. It can be seen that the indoor vibration isolation has remarkable effect. The vibration isolation at the midspan position is 16 dB, and the vibration isolation at the junction is between 10 and 12.4 dB. The isolation effect of each frequency band is shown in Figure 15. As can be seen, the vibration isolation effect of the midspan and the wall-floor junction mainly occurs in the frequency band of 40~80 Hz. The vibration isolation at the midspan position in each frequency band is higher than that at wall-floor junctions. The vibration isolation under 10 Hz in the low-frequency band is reduced, and the difference in vibration isolation between the two positions is small.

6. Conclusions

In this paper, theoretical calculation, field measurement, and numerical simulation are used to analyze the effect of indoor vibration isolation. The major findings are drawn as follows:

- (1) After adopting the vibration damping scheme, the maximum acceleration level of 1/3 octave with a center frequency of 50 Hz is 38 dB lower than the corresponding limit (86 dB) in Standards for Indoor Vibration Limits and Measurement Methods for Residential Buildings (GB/50355-2005) (Level 1 daytime limit). As can be seen, this method improves the vibration isolation effect obviously in the frequency range with 50 Hz as the center, and the effect at the midspan position is better than that at wall-floor junctions.
- (2) By comparing the effects before and after isolation, the following has been found: (1) in indoor rooms,

the vertical isolation of the midspan increases with the floor height, while it is opposite for the wall-floor junction; (2) in kitchen rooms, the vertical isolation of the midspan and the junction decreases as the floor height increases; and (3) in bathrooms, the vertical isolation of the midspan and junction increases with the floor height. On each floor, the vibration levels of different positions in the room are obviously different. For indoor rooms with a large span and kitchens and bathrooms with a small span, the isolation level of the midspan is greater than that of the junction. The span has no obvious impact on the difference in the isolation level of each floor, and the same is true for the floor material.

- (3) The isolation effect is directly proportional to the total thickness of the vibration isolation system, and the system of concrete filling material has the best effect. The stiffness of the isolator is inversely proportional to the effect. The smaller the stiffness, the better the isolation effect, which is mainly concentrated in the range of 40~80 Hz.
- (4) The optimized parameters are applied to Room SN2 with remarkable results. The vibration reduction at the midspan is 16 dB, and the vibration isolation at wall-floor junctions is between 10 and 12.4 dB. With its convenient construction technology, short cycle, and low cost, the method has wide application prospects especially for existing buildings.

Data Availability

All data used to support the findings of this study are included within the supplementary information files. Details can be found in annex 2.

Conflicts of Interest

The authors declare that they have no conflicts of interest.

Acknowledgments

This work was supported by the National Natural Science Fund (51708450), China Postdoctoral Science Foundation Project (2018M643702), Basic Research Project of Natural Science in Shaanxi Province (2018JQ5169), Shaanxi Provincial Postdoctoral Foundation Project (2018BSHEDZ Z22), Ph.D. Research Start-Up Project (107-451115002), and School-Level Scientific Research Project (2016CX025).

References

- [1] W. N. Liu and M. Ma, *Metro Train Induced Environmental Vibrations: Prediction, Evaluation and Control*, Science Press, Beijing, China, 2013.
- [2] M. Ma, W. N. Liu, D. Y. Ding et al., "Prediction of influence of metro trains induced vibrations on sensitive instruments," *Journal of Vibration and Shock*, vol. 30, no. 3, pp. 185–190, 2011.
- [3] S. J. Li, M. L. Lou, J. M. Ding et al., "Analysis of floating floor isolation for subway induced vibration," *Structural Engineers*, vol. 23, no. 5, pp. 10–14, 2007.

- [4] H. L. Zhang, X. Yan, and H. B. Su, "Experimental study of vibration isolation performance on "room in room" structure," *Experimental Technology and Management*, vol. 25, no. 6, pp. 45–49, 2008.
- [5] T. Y. Wang, Z. Zhang, and J. M. Ding, "Study on vibration and noise control of Shanghai symphony orchestra music hall," *Environmental Engineering*, vol. 30, no. S1, pp. 13–18, 2012.
- [6] Z. G. Yin, *Environmental Vibration and Noise Induced by Railways*, Tongji University, Shanghai, China, 2008.
- [7] W. Zhou, Y. Wu, W. Qu et al., "The research of indoor vibration isolation of existing building in the environment of urban rail transit system," *Industrial Construction*, vol. 38, no. S1, pp. 307–311, 2008.
- [8] Q. Xia and W. J. Qu, *Study on Subway-Induced Existing Building Vibration and Isolation Method*, Tongji University, Shanghai, China, 2014.
- [9] Q. Xia, W. J. Qu, and X. Shang, "Test for effects of metro train-induced vibration on existing masonry buildings," *Journal of Vibration and Shock*, vol. 32, no. 12, pp. 11–16, 2013.
- [10] Q. Xia and W. J. Qu, "Experimental and numerical studies of metro train-induced vibrations on adjacent masonry buildings," *International Journal of Structure Stability and Dynamics*, vol. 16, pp. 1550067–1550094, 2017.
- [11] P. Chen, Z. H. Huang, and Q. B. Jiang, "Study on dynamic and static stiffness ratio of damping rubber," *Special Purpose Rubber Products*, vol. 33, no. 6, pp. 37–40, 2012.
- [12] National Standards of the People's Republic of China, *Indoor Vibration Limits of Residential Buildings and Standards of Measurement Methods*, China Construction Industry Publishing House, Beijing, China, 2005.
- [13] Q. Xia and W. J. Qu, "Numerical analysis on metro train-induced vibrations and their influences and affecting factors on existing masonry building," *Journal of Vibration and Shock*, vol. 36, no. 6, pp. 189–194, 2014.



Hindawi

Submit your manuscripts at
www.hindawi.com

